Research Article
Open Access
CrossMark

Study of crystallization phases and magnetic properties of $Fe_{72.5}Cr_1Nb_3Cu_1Si_{13.5}B_9$ nanocrystalline alloy prepared by rapid quenching method

Abstract

Phase constitution and soft magnetic properties of nanocrystalline alloy of composition $Fe_{72.5}Cr_1Nb_3Cu_1Si_{13.5}B_9$ prepared by single roller rapid quenching technique was investigated in this paper. The amorphous nature and the nanocrystal formation of the alloy was determined by X-ray diffraction (XRD) besides the crystallization kinetics was studied by Differential Thermal Analysis (DTA). The annealing temperature was maintained within the range 450°C to 800°C for 30minutes. DTA study reveals the existence of two exothermic peaks one for primary crystallization of á – Fe(Si) phase and other for secondary crystallization of Fe_2B phase. The temperature difference between two crystallization peaks is found to exist ~170°C. This large temperature gap is an indication of the enhancement of stability of á – Fe(Si phase against detrimental Fe_2B phase. In the optimized annealing condition, the grain size has been obtained in the range of 10-15 nm. The saturation magnetization (M_s) has been observed 128 Am^2/kg. In as-prepared condition Curie temperature (T_c) was found 316°C, close compared to the T_c of original FINEMET. Thus, a slight substitution (1 atomic %) of iron (Fe) by chromium (Cr) in original FINEMET enhances the thermo-magnetic stability of the alloy.

Keywords: FINEMET, DTA, á – Fe(Si) phase, Curie temperature, saturation magnetization

Volume 4 Issue 2 - 2020

Shihab MT,[1] RezaMA,[2] Shil SK,[1] Tawhid MM,[1] Sikder SS,[1] Gafur MA[3]

[1]Department of Physics, Khulna University of Engineering & Technology, Bangladesh
[2]Nuclear Power Plant Company Bangladesh Limited (NPCBL), Bangladesh
[3]Bangladesh Council of Scientific and Industrial Research, Bangladesh

Correspondence: Shihab MT, Department of Physics, Khulna University of Engineering & Technology, Khulna, Bangladesh, Email md.tahmid.shiha@gmail.com

Received: January 12, 2020 | **Published:** March 02, 2020

Abbreviations: XRD, X-ray diffraction; RAM, random anisotropy model; Nb, Niobium

Introduction

In 1988 Yoshizawa, Oguma and Yamauchi at Hitachi Metals Ltd. developed the first nanocrystalline ultra-soft magnetic alloy called FINEMET having a composition $Fe_{73.5}Nb_3Cu_1Si_{13.5}B_9$ by adding Copper (Cu) and Niobium (Nb) to Fe-Si-B amorphous alloys.[1] This newly developed material is cost effective and exhibits splendid soft magnetic properties. The FINEMET consists of a two-phase microstructure in its optimally annealed condition. This microstructure is made up of a ferromagnetic bcc á – Fe(Si) phase and/or a DO_3 type of ordered Fe(Si) phase with the grain size of 10-25 nm embedded homogeneously in this residual ferromagnetic amorphous matrix. These represent a new family of excellent soft magnetic behavior: high saturation magnetization (~1.2T), low coercivity (≤1Am^{-1}), high relative magnetic permeability (≥10^4) and have stimulated an enormous research activity due to their potential applications.[2–9] The formation of the particular FINEMET structure can be attributed to the combined effects of Cu and Nb and their low solubility in bcc Fe. Cu is thought to promote the nucleation of Fe(Si) grains while Nb and Boron (B) inhibit the grain growth and accelerate the formation of ferromagnetic Fe-B phases,[10] which are detrimental for the soft magnetic properties. The nanoscale grain with magnetic softness can be understood in the framework of the random anisotropy model (RAM) proposed by Alben et al.[11] According to the RAM, extraordinary soft magnetic properties of nanocrystalline materials arise from strong inter-granular magnetic coupling, the suppression of effective magnetocrystalline anisotropy and vanishing magnetostriction. The magnetocrystalline anisotropy vanishes when the grain size is smaller than the ferromagnetic exchange length and magnetostriction approaches zero due to the cancellation of the positive magnetostriction of á – Fe(Si) crystallites and negative magnetostriction of the amorphous matrix. Effect of partial substitution of Fe with Co,[12,13] Al[14,15] Al-Ge,[16] Ni,[17] Cr-Mo[18] and Cr[19] have been investigated. It has been reported that the replacement of Fe by Cr enhances the thermal stability against crystallization and reduces the Curie temperature (T_c) of the amorphous phase.[19] This gives the opportunity of studying the magnetic interaction in a wider temperature range between the T_c of the amorphous phase and that of the nanocrystalline phase. The magnetocrystalline Cr substituted Fe-based metallic glasses has been the subject of intensive research not only for the promising technological applications but the co-existence of various magnetic phases at an elevated temperature which make them attractive for studying basic magnetic phenomena.[20–22] The main theme of the present paper is to synthesize Fe-based alloy of $Fe_{73.5}Nb_3Cu_1Si_{13.5}B_9$ composition in the amorphous state by using rapid quenching technique and study the formation of different phases by varying annealing temperature (T_a). The evolution of nanograins and the magnetic properties in the as-prepared condition are also investigated.

Experimental

Melt spinning is a widely used production method for rapidly solidifying materials as well as preparing amorphous metallic ribbons.[23–26] In order to prepare amorphous $Fe_{73.5}Nb_3Cu_1Si_{13.5}B_9$ alloys, the melt spinning facilities were used at the Centre for Materials Science, National University of Hanoi, Vietnam. Amorphous ribbons with the composition $Fe_{73.5}Nb_3Cu_1Si_{13.5}B_9$ were prepared in an arc furnace on a water-cooled copper hearth under an atmosphere of pure Argon (Ar). The source materials were Fe (99.9%), Cr (99.9%), Nb (99.9%), Cu (99.9%), Si (99.9%) and B (99.9%) obtained from

Johnson Matthey (Alfa Aesar Inc.). The required amounts of the constituent elements were taken from pure metal bars or flakes weighed with a sensitive electronic balance and placed on the copper hearth inside the arc furnace. The furnace chamber was first evacuated (10^{-4} torr) and flushed with Ar gas. The process was performed several times to remove residual air and finally, the furnace chamber was kept in an Ar atmosphere. The arc melted master alloy was crashed into small pieces and put inside the quartz tube crucible for re-melting by induction furnace using a medium frequency generator with the maximum power of 25kW at a suitable frequency of 10kHz. The molten alloy was vertically ejected onto the wheel surface. The master alloy sample was inductively remelted inside the quartz tube crucible followed by ejecting the molten metal with an overpressure of 250 mbar of 99.9% pure Ar supplied from an external reservoir through a nozzle onto a rotating copper wheel with the surface velocity of 30 m/sec. The temperature was observed by an external pyrometer from the top surface of the molten alloy through a quartz window. The metal alloys were removed at a temperature of about 150 to 250K above the melting point of the alloy to have uniform thickness and to reduce the roughness of both sides of the ribbon. The resulting ribbon samples had a thickness of about 20-25μm and a width ~6mm. Crystallization phase analysis was carried out by Differential Thermal Analysis (DTA) (SEIKO TG/DTA 6300). The crystallization activation energies for primary and secondary phases have been calculated using Kissinger's equation:[27] $E = -kT_p \ln\left(\frac{\hat{a}}{T_p^2}\right)$ where β is the heating rate, T_p is the crystallization peak temperature, E is the activation energy and k is the Boltzmann's constant. The Nanocrystalline structure has been observed by XRD (Philips (PW 3040) X 'Pert PRO XRD) with Cu-K_α radiation. Lattice parameter (a_0) was calculated from diffraction peaks in XRD patterns. Grain size (D_g) of all annealed samples was determined using the Debye-Scherrer method.[28] Si contents were computed using the equation:[29] $X = \frac{(a_0 - 2.8812)}{0.0022}$, where X is at.% Si in the nano grains. Magnetic properties such as field dependent magnetization and temperature dependent magnetization were measured by a vibrating sample magnetometer (VSM) (880 DMS, USA).

Results and discussion

DTA Results

Figure 1A-1F represents the DTA traces of as-cast $Fe_{73.5}Nb_3Cu_1Si_{13.5}B_9$ alloy from room temperature to 800°C with heating rates of 10–60°C/min at the step of 10°C. In each figure, two exothermic peaks are distinctly observed; corresponding to two different crystallization events initiated at temperature T_{x1} and T_{x2} respectively. Figure 1 reveals that the crystallization of each phase occurs over a wide range of temperatures and the peak temperature shifts to higher values with the increase of heating rate. In other word, more heat energy is required for the formation of crystalline phases with increasing heating rates. From each of the DTA traces, it is obvious that the area under the first crystallization peak is larger than the area covered by the second crystallization peak.

Figure 1 also shows that the two crystallization events are separated by a large temperature gap of ~170°C. For FINEMET without Cr the temperature difference between two events was found ~150°C.[30] This implies that a slight Cr-content has weakened the diffusion process to form the crystallization phases since Cr has a melting temperature (1857°C) higher than that of Fe (1536°C). The large separation between two crystallization events is one of the characteristic features of the FINEMET type-alloys, which exhibit easy nano crystallization.[31] The activation energy of á – Fe(Si) and Fe_2B phases has been calculated using Kissinger's plot shown in Figure 2A & 2B respectively. It shows that thermal crystallization activation energy of á – Fe(Si) phase is 3.26eV and Fe_2B phase is 4.87eV respectively. The activation energy for formation of á – Fe(Si) phase is approximately similar to that for the original FINEMET (3.25eV).[32] It is also noticed that the activation energy for first crystallization phase is lower than the second crystallization phase. This is because, at the early stage of crystallization, a formation of Cu clusters leads to low activation energy for preferential nucleation however, with the increase of crystallized volume fraction, the Cu-rich regions gradually run out.[33] The data for the as-cast $Fe_{73.5}Nb_3Cu_1Si_{13.5}B_9$ alloy with heating rates are enlisted in Table 1. DTA traces for a constant heating rate of 20°C/min of the $Fe_{73.5}Nb_3Cu_1Si_{13.5}B_9$ alloy in the annealed state at different temperatures are shown in Figures 3A-3C. We observe from Figures 3A that as the annealing temperature (450°C) is lower than the first crystallization temperature, the onset crystallization temperature is almost unchanged with respect to its amorphous precursor. But when annealed at 550°C and 600°C which are higher than the onset of crystallization temperature of T_{x_1} (531°C), the primary crystallization peak has completely diminished and display diffused character meaning that substantial amount of primary crystallization, á – Fe(Si) phase has already been completed. The 2nd peak in Figures 3A-3C does not show any significant changes since the T_a is low compared to T_{x2} . Results of the DTA scan of the sample of as-cast and annealed at different temperatures are tabulated in Table 2.

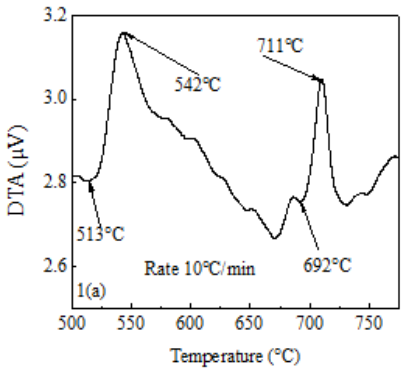

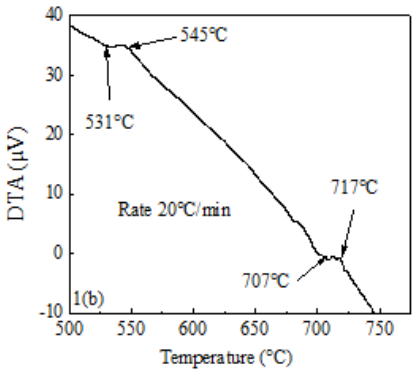

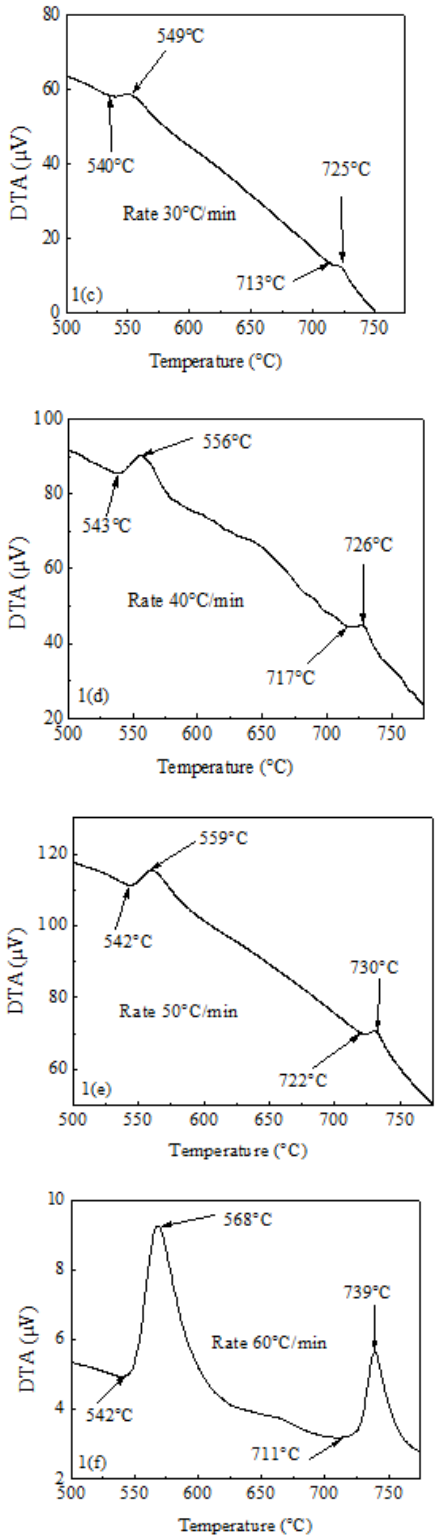

Figure 1 DTA traces of as-cast $Fe_{72.5}Cr_1Nb_3Cu_1Si_{13.5}B_9$ alloy with the heating rates of (A) 10°C/min, (B) 20°C/min, (C) 30°C/min, (D) 40°C/min, (E) 50°C/min and (F) 60°C/min.

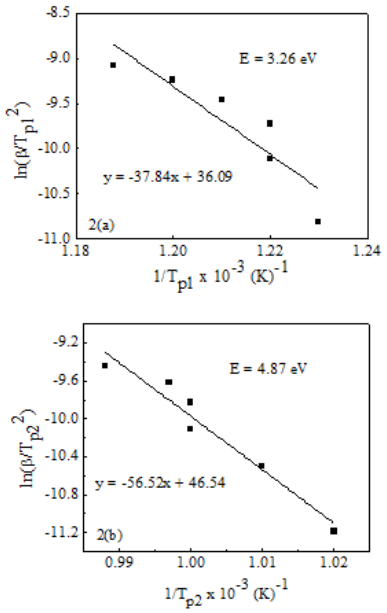

Figure 2 Kissinger's plot to determine the activation energy of (A) $\alpha - Fe(Si$ phase and (B) Fe_2B phase of the $Fe_{72.5}Cr_1Nb_3Cu_1Si_{13.5}B_9$ alloy.

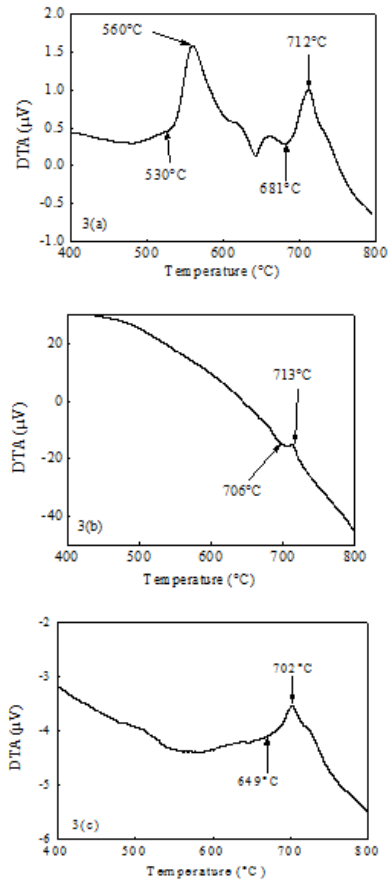

Figure 3 DTA traces of $Fe_{72.5}Cr_1Nb_3Cu_1Si_{13.5}B_9$ alloy at the heating rate of 20°C/min annealed at (A) 450°C (B) 550°C and (C) 600°C.

Citation: Shihab MT, Reza MA, Shil SK, et al. Study of crystallization phases and magnetic properties of $Fe_{72.5}Cr_1Nb_3Cu_1Si_{13.5}B_9$ nanocrystalline alloy prepared by rapid quenching method. *Material Sci & Eng.* 2020;4(2):37–43. DOI: 10.15406/mseij.2020.04.00124

Table 1 Effect of heating rate on 1st and 2nd crystallization of $Fe_{72.5}Cr_1Nb_3Cu_1Si_{13.5}B_9$ alloy

Heating rate, β (°C/min)	1st starting cc (°C)	1st Peak T_{p_1} (°C)	2nd starting T_{x_2} (°C)	2nd Peak T_{p_2} (°C)	Peak separation temperature (°C)	Activation energy of 1st crystallization (eV)	Activation energy of 2nd crystallization (eV)
10	513	542	692	711	169		
20	531	544	707	717	173		
30	540	549	713	725	176		
40	543	556	717	726	170	3.26	4.87
50	542	559	722	730	171		
60	542	568	711	739	171		

Table 2 Annealing effects on 1st and 2nd crystallization states of the $Fe_{72.5}Cr_1Nb_3Cu_1Si_{13.5}B_9$ alloy at a constant heating rate of 20°C/min

T_a (°C)	T_{x_1} (°C)	T_{p_1} (°C)	T_{x_2} (°C)	T_{p_2} (°C)	Peak separation temperature (°C)
As-cast	531	545	707	717	172
450	530	560	681	712	152
550	--	--	706	713	--
600	--	--	649	702	--

Structural Analysis by XRD

XRD patterns for the $Fe_{73.5}Nb_3Cu_1Si_{13.5}B_9$ alloy as as-cast state and annealed at temperature 450, 500, 550, 600, 650, 700, 750 and 800°C each for 30 minutes are presented in Figure 4A. It is evident that the XRD patterns for the samples at as-cast state and annealed below 500°C, i.e. at 450°C, exhibit only one broad peak around 2θ = 45°C, at the position of d_{110} reflection which is generally referred to as diffuse hallow, indicative of an amorphous phase. This suggests that at T_a<500°C, the alloy remains amorphous. So the onset crystallization temperature determined from these results is between 450-500°C. The crystallization onset temperatures from DTA experiment for different heating rates were found in the range of 513-543°C, which shows a good consistency with the XRD results. The value of FWHM for the sample annealed at 550°C is 0.8144. With increasing T_a beyond 550°C, the FWHM value is getting smaller. It confirms that the crystallization occurs to a good extent at the higher T_a. The XRD pattern illustrated in Figure 4(a) reveals that the both the position and broadness of the (110) diffraction peak vary as the annealing temperature increases. We observe a general increase in the intensity of the diffraction peak with the annealing temperature, consistent with an increase in the crystalline volume fraction. The existence of Fe_2B phase is noticed in the XRD spectra when the sample annealed above 700°C which is in agreement with the crystallization temperature obtained by DTA curves. Li-xia Wen et al.[34] also reported the similar result.[34] The slight shift of peak towards the lower/higher angles with increasing T_a has been noticed in the XRD spectra as shown in Figure 4B. This may be related with stress i.e., when first crystallizes at ~500°C there is stress build up, with increasing annealing temperature the stress relaxes; then it comes to a second crystallization stage at ~700°C and stress builds up again. As a result, a change in the value of a_0 as well as Si-content in the á – Fe(Si) phase with increasing T_a are obtained. The values of FWHM, a_0 , D_g, and Si-content are enlisted in Table 3. Figure 5 shows that in the T_a range of 500 to 700°C, the grain size remains in the range of 10 to 15nm, corresponding to a soft magnetic á – Fe(Si) phase. Above 700°C grain grow rapidly and attain a maximum value of 32 nm at 800°C indicating the formation of the Fe_2B phase. These results suggest that within the annealing temperature range of 500-700°C, the alloy maintain its nanocrystalline structure with a nominal grain size of <15nm. Hence in order to obtain the non acrystalline alloy with optimum soft magnetic properties annealing has to be carried out within this critical temperature.

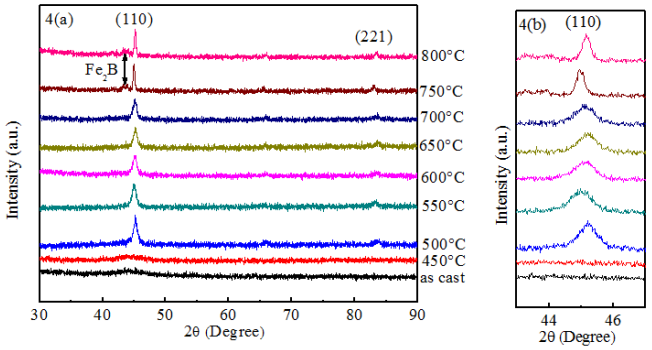

Figure 4 (A) XRD spectra of $Fe_{72.5}Cr_1Nb_3Cu_1Si_{13.5}B_9$ alloy for as cast and for different annealing temperatures (B) shifting of peak position in the XRD spectra.

Table 3 Experimental XRD data of nanocrystalline $Fe_{72.5}Cr_1Nb_3Cu_1Si_{13.5}B_9$ alloy at different T_a

T_a (°C)	θ (deg.)	d (Å)	FWHM (deg.)	a_0 (Å)	D_g (nm)	Si (at. %)
450	--	--	--	--	--	--
500	22.60	2.006	0.6585	2.8369	15	18
550	22.50	2.020	0.8144	2.8560	11	9
600	22.58	2.012	0.7278	2.8454	13	14
650	22.62	1.997	0.7162	2.8242	14	24
700	22.54	2.009	0.6871	2.8412	14	16
750	22.48	2.012	0.3175	2.8454	28	14
800	22.58	2.008	0.2946	2.8397	32	17

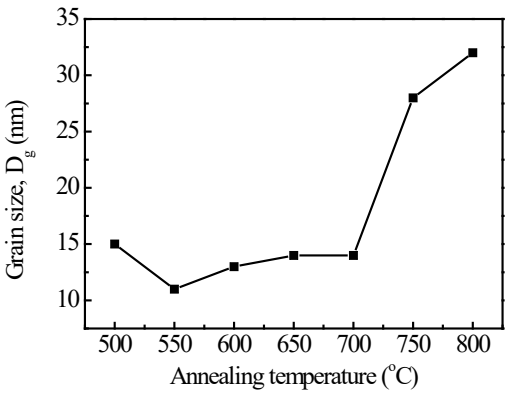

Figure 5 Change of Grain Size with annealing temperature for the $Fe_{72.5}Cr_1Nb_3Cu_1Si_{13.5}B_9$ alloy.

Temperature dependence of specific magnetization

Figure 6A shows the variation of magnetization (M) of $Fe_{73.5}Nb_3Cu_1Si_{13.5}B_9$ alloy in the as-cast state with temperature at constant magnetic field 800 kA/m. It is clearly observed that the magnetization (M) of the sample decreases gradually at low-temperature (<300°C) and falls faster nearer to the T_c of ~316°C. The T_c has been determined as the temperature corresponding to inflection point where the rate of change of M with respect to temperature is maximum shown in Figure 6B. As the temperature approaches T_c, M falls more rapidly near to zero as the thermal energy exceeds the magnetic ordering or the exchange energy. The sharp fall of M at T_c indicates that the material is quite homogeneous from the point of amorphousity. Our measured T_c of 316°C is similar to value reported for the original FINEMET without Cr.[35]

Magnetic field dependence of magnetization

The magnetization process of the $Fe_{73.5}Nb_3Cu_1Si_{13.5}B_9$ alloy in the as-cast state with an applied magnetic field at room temperature is shown in Figure 7. It is clearly evidenced that the magnetization saturates in the amorphous state with a very small applied field of 4×10^4 A/m which is an indication of soft magnetic behavior. For the original FINEMET the saturation magnetization (M_s) of ~150 Am^2/kg at room temperature has been reported.[36] In the present study with the partial substitution of Fe magnetic moment by non-magnetic Cr, we observe that M_s decreases slightly to ~128Am^2/kg.

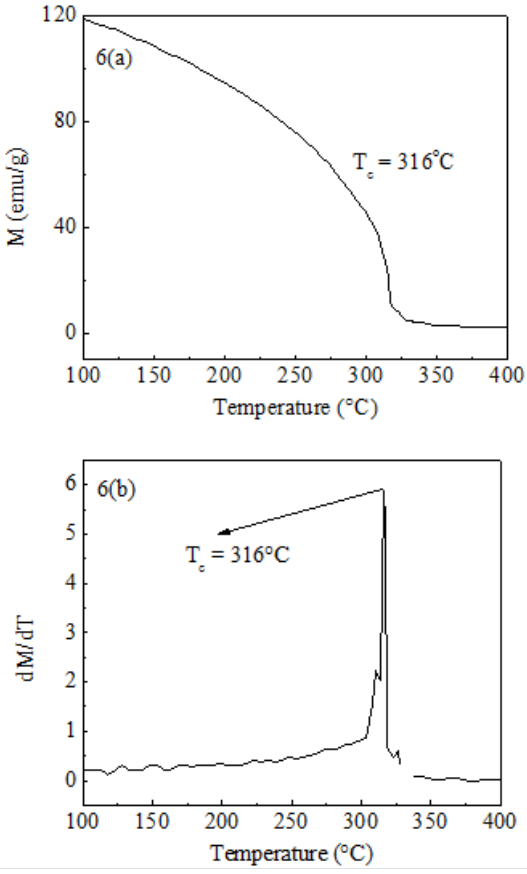

Figure 6 (A) Temperature dependence of specific magnetization (B) $\frac{dM}{dT}$ versus temperature curve of $Fe_{72.5}Cr_1Nb_3Cu_1Si_{13.5}B_9$ alloy.

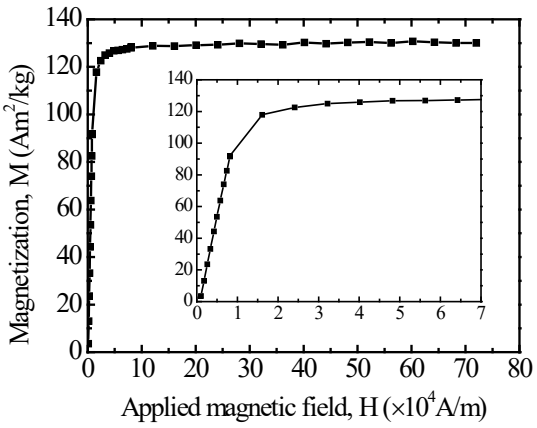

Figure 7 Magnetization curve for the Fe72.5Cr1Nb3Cu1Si13.5B9 alloy with applied magnetic field.

Conclusion

In this work the $Fe_{73.5}Nb_3Cu_1Si_{13.5}B_9$ alloy has been synthesized by the substitution of Fe with small amount of Cr (1 atomic %) in the original FINEMET composition. With the addition of Cr in FINEMET, we found that although the room temperature M_s decreases from ~150 to 128Am²/kg, the T_c of the sample is similar to original FINEMET. Annealing of the amorphous sample in the temperature range of 450 to 800°C reveals that the crystallization onset temperature for the á – Fe(Si) phase is between 450-500°C. The phase has a nanocrystalline nature with crystallite size of <15nm. As the annealing temperature increases, this crystallite size remains relatively constant up to T_a of 700°C. Above 700°C, the crystallites coarsen considerably to 32nm. Two crystallization onsets at ~515 and 700°C are observed from DTA analysis and these onset temperatures are also found to be dependent on the heating rate during the measurement. The activation energy of the primary crystallization of á – Fe(Si) phase is found to be 3.26 eV which is slightly higher than the original FINEMET. A large temperature difference of ~170°C between the two crystallization events is measured. This large temperature gap is an indication of the enhancement of stability of á – Fe(Si) phase against detrimental Fe_2B phase due to a slight substitution of Cr in place of Fe. Our results demonstrate that with the addition of Cr, soft magnetic nanograins in the amorphous alloy with an enhanced thermo-magnetic stability can be obtained at lower heat treatment than the original FINEMET which is good for high quality inductor applications.

Acknowledgements

The authors are highly grateful to Centre for Materials Science, National University of Hanoi, Vietnam for using their laboratory to synthesize the alloys and to Bangladesh Council of Scientific and Industrial Research (BCSIR) for giving their experimental facilities for characterization.

Conflicts of interest

The authors declare that there are no conflicts of interest.

References

1. Yoshizawa Y, Oguma S, Yamauchi K. New Fe-based soft magnetic alloys composed of ultra-fine grain structure. *J Appl Phys*. 1988;64:6044–6046.
2. Hakim MA. Magnetic softening of nanocrystalline FeCuNbSiB alloys on annealing. *J Bangladesh Electronic Society*. 2004;4:4–45.
3. Xing Lao, Yanhui Wu, Mangui Han, et al. High frequency permeability of Fe-Cu-Nb-Si-B nanocrystalline flakes with the distribution of shape anisotropy fields. *J Magn Magn Mater*. 2018;451:5–10.
4. Serikov VV, Kleinerman NM, Volkova EG, et al. Structure and magnetic properties of nanocrystalline FeCuNbSiB alloys after a thermochemical treatment. *Phys Metals Metallogr*. 2006;102:268–273.
5. Sybille Flohrer, Rudolf Schäfer, Giselher Harzer. Magnetic microstructure of nanocrystalline FeCuNbSiB soft magnets. *Journal of Non-crystalline Solids*. 2008;354:5097–5100.
6. Atef Lekdim, Laurent Morel, Marie-Ange Raulet. Effect of the remaining magnetization on the thermal ageing of high permeability nanocrystalline FeCuNbSiB alloys. *J Magn Magn Mater*. 2018;460:253–262.
7. Kane SN, Sarabhai S, Gupta A, et al. Effect of quenching rate on crystallization in $Fe_{73.5}Nb_3Cu_1Si_{13.5}B_9$ alloy. *J Magn Magn Mater*. 2000;215-216:372-374.
8. Saha DK, Hakim MA. Crystallization Behaviour of $Fe_{73.5}Nb_3Cu_1Si_{13.5}B$. *Bang J Acad Sci*. 2006;30(2):177–187.
9. Okumura H, Laughlin DE, McHenry ME. Magnetic and structural properties and crystallization behavior of Si-rich FINEMET materials. *J Magn Magn Mater*. 2003;267:347–356.
10. Yoshizawa Y, Yamauchi K. Fe-Based Soft Magnetic Alloys Composed of Ultrafine Grain Structure. *Materials Transjaction JIM*. 1990;31(4):307–314.
11. Alben R, Becker JJ, Chi MC. Random anisotropy in amorphous ferromagnets. *J Appl Phys*. 1978;49(3):1653–1658.
12. Ohnuma O, Pins DH, Abe T, et al. Optimization of the microstructure and properties of Co-substituted Fe-Si-B-Nb-Cu nanocrystalline soft magnetic alloys. *Appl Phys*. 2003;93(11):1986–9194.
13. Fernandez A, Perez MJ, Tejedor M. Thermomagnetic analysis of amorphous $(Co_xFe_{1-x})_{73.5}Nb_3Cu_1Si_{13.5}B_9$ metallic glasses. *J Magn Magn Mater*. 2000;22:338–344.
14. Zorkovska A, Kovac J, Sovak P, et al. Structure and Magnetic behavior of Fe-Cu-Nb-Si-B-Al alloys. *J Magn Magn Mater*. 2000;215-216:492–494.
15. Lim SH, Pi WK, Noh TH, et al. Effects of Al on the magnetic properties of nanocrystalline $Fe_{73.5}Nb_3Cu_1Si_{13.5}B$ alloys. *J Appl Phys*. 1993;73(10):6591–6593.
16. Shahri F, Beitollahi A, Shabestari SG, et al. Structural characterization and nanocrystalline AlGe-substituted FeSiBNbCu ribbons. *J Magn Magn Mater*. 2007;312:35–42.
17. Iturriza N, Fernández L, Ipatov M, et al. Nanostructure and magnetic properties of Ni-substituted finemet ribbons. *J Magn Magn Mater*. 2007;316:e74–e77.
18. del Riego L, M El Ghannami, Dominguez M, et al. Superparamagnetic behavior of a nanocrystalline Fe(Cr-Mo)SiBCuNb alloy. *J Magn Magn Mater*. 1999;197:201–203.
19. Franco V, Conde CF, Conde A. Magnetic properties and crystallization of a $Fe_{73.5}Nb_3Cu_1Si_{13.5}B$ alloy. *J Magn Magn Mater*. 1999;203:60–62.
20. Moya JA. Improving soft magnetic properties in FINEMET-like alloys. A study. *J Alloys and Compd*. 2015;622:635–639.
21. Kun Peng, Ling Tang, Yingwei Wu. Evolution of microstructure and magnetic properties of $Fe_{73.5}Si_{13.5}B_9Nb_3Cu_1$ amorphous alloy during ion bombardment process. *J Magn Magn Mater*.460 (2018):297–301.

22. Tsepelev T, Yu Starodubtsev, Konashkov V, et al. Thermomagnetic analysis of soft magnetic nanocrystalline alloys. *J Alloys and Compd*. 2017;207:210–213.

23. Müller M, Matern N. The influence of refractory element additions on the magnetic properties and on the crystallization behavior of nanocrystalline soft magnetic Fe-B-Si-Cu alloys. *J Magn Magn Mater*. 1994;136:79–87.

24. Mondal SP, Maria KH, Sikder SS, et a. Influence of Annealing Conditions in Nanocrystalline and Ultra-soft Magnetic properties of $Fe_{73.5}Cu_1Nb_3Si_{13.5}B_9$. *J Mater Sci Technol*. 2012;28(1):21–26.

25. Premkumar Murugaiyan, Anand Abhinav, Rahul Verma, et al. Influence of Al addition on structural, crystallization and soft magnetic properties of DC Joule annealed FeCo based nanocrystalline alloys. *J Magn Magn Mater*. 2018;448:66–74.

26. Tho ND, Chau N, Yu SC, et al. Soft magnetic behaviour in amorphous and nanocrystalline $Fe_{73.5-x}Mn_xSi_{13.5}B_9Nb_3Cu_1$ (x=1, 3, 5) alloys. *J Magn Magn Mater*. 2006;304(2):868–870.

27. Kissenger HE. Variation of Peak Temperature with Heating Rate in Differential Thermal Analysis. *J Res Nat Bur Stand*. 1956;57:217–221.

28. Culity BD. Elements of X-Ray Diffraction. London, England. Wesley publishing company, Inc.; 1959: 262.

29. Bozoroth RM. Ferromagnetism D. Princeton, New jersey. Van Nostrand company Inc; 1968:74.

30. Leu MS, Chin TS. Crystallization behavior and temperature dependence of the initial permeability of an FeCuNbSiB alloy. *J Appl Phys*. 1997;81:4051–4053.

31. Pozo López G, Fabietti LM, Condó AM, et al. Microstructure and soft magnetic properties of Finemet-type ribbons obtained by twin-roller melt-spinning. *J Magn Magn Mater*. 2010;322:3088–3093.

32. Chau N, Hoa NQ, Luong NH. The crystallization in Finemet with Cu substituted by Ag. *J Magn Magn Mater*. 2005;290–291:1547–1550.

33. Liu T, Chen N, Xu ZX, et al. The amorphous-to-nanocrystalline transformation in $Fe_{73.5}Cu_1Nb_3Si_{13.5}B_9$ studied by thermogravimetry analysis. *J Magn Magn Mater*. 1996;152:359–364.

34. Li-xia Wen, Zhi Wang, Jia Wang, et al. High temperature magnetic permeability of Si-rich Finemet-type nanocrystalline $(Fe_{1-x}Co_x)_{74.5}Nb_2Si_{17.5}B_5Cu_1$ alloys. *J Magn Magn Mater*. 2015;379:265–269.

35. Knobel K, Sinnecker JP, Sato Turtelli R, et al. The influence of quenching rate on magnetic properties of amorphous ribbons. *J Appl Phys*. 1993;73(10):6603–6605.

36. Lovas A, Kiss LF, Balong L. Saturation magnetization and amorphous Curie point changes during the early stage of amorphous nanocrystalline transformation of a FINEMET-type alloy. *J Magn Magn Mater*. 2000;215-216:463–465.

Citation: Shihab MT, Reza MA, Shil SK, et al. Study of crystallization phases and magnetic properties of $Fe_{72.5}Cr_1Nb_3Cu_1Si_{13.5}B_9$ nanocrystalline alloy prepared by rapid quenching method. *Material Sci & Eng.* 2020;4(2):37–43. DOI: 10.15406/mseij.2020.04.00124